minerals

MDPI

Article

Brine–Melts and Fluids of the Fe-F-P-(Ba)-(Sr)-REE Central Asian Carbonatite Province (Southern Siberia and Mongolia): The Petrogenetic Aspects

Ilya Prokopyev [1,2,3,*], Anna Doroshkevich [1,2,4], and Anna Redina [2,3]

[1] Geology and Geophysics Department, Novosibirsk State University, Pirogova Street 1, 630090 Novosibirsk, Russia
[2] V.S. Sobolev Institute of Geology and Mineralogy, Siberian Branch of the Russian Academy of Sciences, Akademika Koptyuga Avenue 3, 630090 Novosibirsk, Russia
[3] Tuvinian Institute for Exploration of Natural Resources, Siberian Branch of the Russian Academy of Sciences, St. Internatsionalnaya, 117 A, 667007 Kyzyl, Russia
[4] Dobretsov Geological Institute, Siberian Branch of the Russian Academy of Sciences, St. Sakhyanova 6a, 670031 Ulan-Ude, Russia
* Correspondence: prokop@igm.nsc.ru; Tel.: +7-913-387-8321

Abstract: The carbonatite complexes of the Central Asian carbonatite province comprise the Siberian carbonatites of the Western Transbaikalia and the Central Tuva regions, as well as those from the Mushugai-Khudag complex in Southern Mongolia. They are confined to Late Mesozoic rift structures and have endured considerable tectono-magmatic processes caused by intense plume activity, which also accompanied their formation. A systematic study of melt and fluid inclusions revealed that these carbonatites formed as a result of immiscibility processes in silicate–carbonate (salt) melts, as well as fractional crystallization. Alkaline–carbonatite rocks crystallized in the presence of brine–melts with different compositions, i.e., alkaline–fluorine, carbonate, sulfate, phosphate, and chloride. These melts are responsible for mineralization during the orthomagmatic stage and the primary phase of Fe-F-P-(Ba)-(Sr)-REE ore formation at temperature ranges of 850–830 °C, 650–610 °C, and 560–440 °C and pressures between 290 and 350 MPa. At a later stage, the brine–melts evolved into saline hydrothermal fluids, which are considered to be the source of the second stage of F-(Ba)-(Sr)-REE ore mineralization. The saline crystal–fluid inclusions consist mainly of fluorine–sulfate–carbonate–chloride and bicarbonate–chloride compositions, with temperatures of approximately 480–250 °C and pressures below 250 MPa. The shift from melt to fluid in carbonatite complexes could occur more frequently in nature than previously believed and could also apply to other F-REE carbonatite complexes that are linked to rifting and plume activity in mountain-building zones.

Keywords: melt and fluid inclusion; brine–melts; Late Mesozoic; Fe-F-(Ba)-(Sr)-REE; carbonate–silicate immiscibility; carbonatites; Central Asian Carbonatite Province

Citation: Prokopyev, I.; Doroshkevich, A.; Redina, A. Brine–Melts and Fluids of the Fe-F-P-(Ba)-(Sr)-REE Central Asian Carbonatite Province (Southern Siberia and Mongolia): the Petrogenetic Aspects. *Minerals* **2023**, *13*, 573. https://doi.org/10.3390/min13040573

Academic Editor: Paul Bédard

Received: 20 February 2023
Revised: 17 April 2023
Accepted: 18 April 2023
Published: 19 April 2023

1. Introduction

Today, carbonatite complexes represent the main source, and the largest deposits, of a number of strategic elements, such as rare earth elements (REEs), niobium, and zirconium [1–6]. Over 80% of global rare earth deposits are associated with carbonatites and their weathering crusts. In addition, carbonatite complexes are commercially mined for apatite (P), fluorite (F), barium, and strontium. They also contain elevated concentrations of ferrous (Fe, Mn), noble (Au, Ag, Pt), and radioactive (Th, U) elements, as well as industrial reserves of polymetallic (Pb-Zn) ores. Among all carbonatite species, a particular metallogenic type of rare earth carbonatite, Fe-F-P-(Ba)-(Sr)-REE, is recognized. Some

well-known worldwide examples of carbonatite complexes are Bayan Obo, Maoniuping, and Dalucao deposits in China [7,8]; Amba Dongar in India [9]; Kangankunde in Malawi [10]; Okorusu in Namibia [11]; Barra do Itapirapuã in Brazil [12]; and the alkaline–carbonatite complexes of the Central Asian carbonatite province (CACP) that we investigated.

Recent petrological evidence suggests at least three main mechanisms for the origin of carbonatite magmas: (1) partial melting of carbonated mantle [13–15]; (2) long-term fractional crystallization of alkaline–nephelinite magma [16,17]; and (3) silicate–carbonate liquid immiscibility [18–20]. Experimental studies of immiscibility processes of carbonate–silicate melts in the alkaline–nephelinite system have been conducted since the 1960s [21]. The immiscibility phenomenon has been well established in volcanic alkaline rocks, as well as in melt inclusions [19–24]. However, it is worth noting that experimental estimates of the distribution coefficients of elements between immiscible melts have shown that silicate–carbonate immiscibility alone cannot account for the concentration of rare metals in carbonatites [25,26]. Experimental work has also shown that certain agents such as F, S, P, and Cl may contribute to the accumulation of rare earth components in carbonatitic melt at specific PTX parameters, while calcite is acknowledged to largely control the fractionation of REE in the early stages of crystallization [26]. For this particular case, there are also data on the existence of an immiscible hydrous Fe-Ca-P melt in natural samples [27]. Thus, assessing the relevance of both immiscibility and fractional crystallization processes during ore accumulation in carbonatite melts remains a very important petrological task. This study presents a systematic investigation of melt and fluid inclusions in order to identify the mechanisms and conditions of ore genesis in carbonatite systems.

The role of carbonatite fluids in the origin and accumulation of ore elements is of great significance. Evidence of fenitization and other hydrothermal–metasomatic processes is widespread in carbonatite complexes and is typically restricted to ore bodies. Petrological and geothermobarometric observations of fluid inclusions in carbonatite minerals indicate a significant transfer and concentration of rare earth and other ore elements (F, Ba, Sr, P, Fe, Cu, Pb, Zn, etc.) by orthomagmatic (or carbothermal) and hydrothermal fluids [28–30]. In such cases, the main redistribution and concentration of ore elements occurs at a later stage in the evolution of a carbonatite system. Furthermore, mineralogical, fluid inclusion, and experimental studies indicate that REEs are typically concentrated in solutions and crystallize as their own mineral phases due to the remobilization and redistribution of ore components from REE-bearing magmatic mineral phases (e.g., fluorapatite) via orthomagmatic fluids. Subsequently, newly formed hydrothermal ore minerals (e.g., monazite) crystallize [31–37]. Aggressive acidic fluids involved in the transfer and crystallization of ore minerals are highly concentrated (more than 85 wt. %) [37], with a high proportion of cations (Ca, Na, K) and ligands (F, Cl, CO2 (l), SO_4^{2-}). Additionally, the successive evolution of the system involves dilute solutions of predominantly chloride, sulfate, carbonate, and bicarbonate compositions, which are responsible for late ore-bearing hydrothermal mineralization.

The term "brine-melt" was originally introduced by Prokopyev et al. [37] and has been actively used. The brine–melt stage (usually 600–400°C) is commonly referred to as the "magmatic–hydrothermal transition" or "carbothermal stage" [28]; however, we opted for the term "brine-melt" to emphasize the high salinity of the orthomagmatic melts and the solute-deficient volatile exsolution at this stage. In addition, this expression was used to avoid the magmatic/hydrothermal dichotomy inherited from silicate magmatic systems. This continuous transition (evolution) of carbonatite melts into alkaline brine–melts does not rule out the presence of an immiscible aqueous fluid phase [6], which can be highly saline at high-PT conditions [30]. Nonetheless, according to Song et al. [38], REEs are poorly partitioned into this fluid aqueous phase, remaining mainly dissolved in the alkali brine–melt, with the latter being responsible for early magmatic Fe-P-F-REE ore mineralization in the carbonatite complexes.

In the following stages of the evolution of the carbonatite ore-system, the brine–melt

develops into hydrothermal saline fluids (or carbothermal fluids when carbonates are predominant in the solution), where salinity is diluted by increasing the amount of H_2O [30,37]. Fluid inclusions are represented by crystal-brines with evidence of cooling, mixing, and fluid–rock interaction processes.

Fluids of carbonatite origin usually have temperatures of up to 400 °C, whereas external fluids are colder (up to 250 °C) [30,37]. The saline crystal–fluid inclusions are often associated with the second ore-forming stage F-(Ba)-(Sr)-REE in carbonatite systems. Such concentrated fluids contain both residual salt components (Na, K, Ca, Fe, etc.) and ore-elements of the orthomagmatic carbonatite system (Ba, Sr, REE, etc.), acting as aggressive solutions that attack primary magmatic minerals and remove part of the ore components (e.g., REE), hence preventing the formation of new minerals [31–37]. The late stages of the carbonatite system involve dilute solutions that are responsible for late hydrothermal mineralization.

At the time of writing, we have gathered a large enough record of analytical data on melt and fluid inclusions in carbonatites and associated alkaline rocks in the Central Asian Carbonatite Province (CACP) [37,39–42]. Accordingly, in this research, we introduce new information and ideas, which are also derived from modern and early studies, on the origin and evolution of rare earth carbonatites, including their formation mechanisms, as well as relevant changes in the physicochemical properties of minerals and related ore-forming processes. All this is based on a comprehensive geothermobarometric analysis of melts and fluid inclusions.

2. Geological Setting

The carbonatite complexes of the CACP include the Siberian carbonatites of Western Transbaikalia (East Siberia) and Central Tuva regions (South Siberia), as well as those in Southern Mongolia (Figure 1a). They are all part of the Late Mesozoic Central Asian rift structure, the formation of which was accompanied by intense tectono-magmatic processes associated with plume activity [43]. According to recent data, the development of intraplate magmatism during the mid-part of the Early Cretaceous period at the time of approximately 150 (135)–120 Ma has been established, along with the formation of alkaline–carbonatite complexes in the Central Asian fold belt, including carbonatites that are linked to potassium alkaline magmatism [43–45]. The distribution area of these carbonatite bodies is characterized by a variety of correlated silicate igneous rocks, e.g., alkaline and subalkaline gabbroids and syenites, ultramafic alkaline rocks and granitoids, and a few lamprophyres [37,39–52]. Another relevant feature of the Late Mesozoic carbonatite province of Central Asia is its potential reserves and type of ores, given the fact that most carbonatite occurrences belong to the Fe-P-F-(Ba)-(Sr)-REE complex style and yield critical elements in small-size economic occurrences, as well as large deposits.

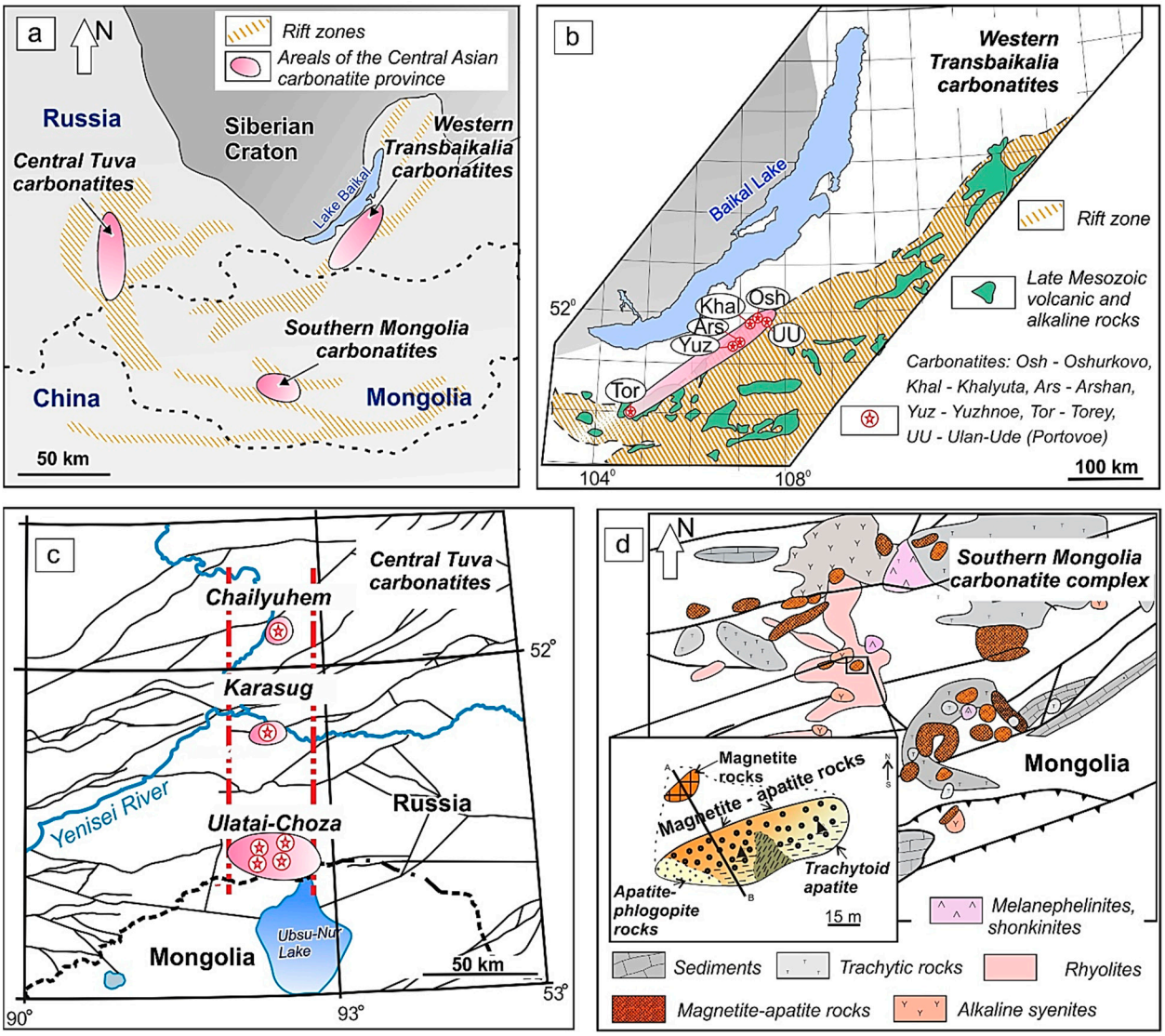

Figure 1. Geological settings of the Central Asian alkaline–carbonatite complexes. (**a**) Location of the carbonatite complexes within the Late-(Middle) Mesozoic rift system of the Central Asian fold belt [51]. (**b**) Simplified geological maps of the Western Transbaikalia carbonatites [52]. (**c**) The Central Tuva carbonatites [37]. (**d**) The Mushugai-Khudag (South Mongolia) alkaline–carbonatite complex [39]. Abbreviations are given according to [53].

Within the Western Transbaikalia paleo-rift zone, a carbonatite province of the same name has been recognized, which includes the Khalyuta, Yuzhnoe, Arshan, Torey, Oshurkovo, and Ulan-Ude (Portovoe) complexes, containing F-Ba-Sr- and REE-bearing occurrences of dolomite–calcite carbonatites [43,45,52] (Figure 1b). Carbonatite complexes are located along the margins of Late Mesozoic rift valleys, forming diatreme, pipe-like, and mantle-like bodies. They are associated with shonkinite and alkaline syenite dikes. Granitic gneisses and quartz syenites (Paleozoic) are the main host rocks for carbonatites, with fenites developing along their contact zones. These rocks were formed within the time period of 130-122 Ma [45]. Detailed information about the geology and mineralogy of these carbonatite complexes is presented in [43,45–47,52,54].

The Southern Siberian Fe-F-REE carbonatites comprise three ore clusters located in the sub-meridional (SN) part of the Central Tuva rift depression, namely, Chailyukhem, Karasug, and Ulatai-Choza (Figure 1c). These carbonatites intrude Early to Middle Paleozoic sandstones, siltstones, limestones, tuffs, conglomerates, and shales, which are confined primarily to fault zones, forming lenses, stocks, pipes, and bodies of complex shapes. The carbonatites were emplaced in two distinct phases, namely, ankerite–calcite

carbonatites (first phase) and siderite carbonatites (second phase). Geological observations suggest that spatially associated igneous rocks in ore-bearing carbonatite clusters correspond to grano-syenite stocks, rare dolerite dikes, lamprophyres (kersantite, spessartite), syenites, and syenite porphyries. Additionally, some ore-bearing carbonatite bodies comprise siderite breccia with fragments of country rocks, associated igneous rocks, and ankerite–calcite carbonatites, which are cemented by a siderite matrix. The age of the Tuva carbonatites is estimated to be between 117 and 119 Ma. The structure and morphology of the pipe-like carbonatite bodies, as well as geological data on melt and fluid inclusions, indicate a fluid-explosive origin [37,43,48,55–57].

The Southern Mongolian area of the CACP is situated in the Gobi Desert and encompasses the Mushugai-Khudag carbonatite–alkaline complex (Figure 1d). The complex comprises nephelinites and alkali feldspar trachytes, which are intersected by stocks and dikes of alkaline syenites, shonkinites, and magnetite–apatite rocks, as well as several small dikes of fine-grained carbonatites [39,49,50]. The country rocks in the area consist of Paleozoic sedimentary–volcanogenic intercalations of limestones, sandstones, argillaceous shales, and mafic effusive rocks, as well as some Carboniferous granitoids. The complex is located within a graben and is confined to a major rift system [49]. In this area, calcite–fluorite rocks form veins and dikes, and some stock-like bodies occur as nearly pure fluorite rocks with a thickness of up to 30 m. Meanwhile, fluorite hydrothermal veins and stock-like bodies are widespread, consisting of fluorite–calcite, fluorite–barite, fluorite–quartz, and fluorite–celestite varieties [39,49,50]. Two independent stocks of ore-bearing apatite and magnetite–apatite rocks are present in the area (Figure 1d). The age of the magnetite–apatite rocks is estimated to be within the range of 138-121 Ma [49].

3. Analytical Methods

Core and rock samples from alkaline–carbonatite complexes of the CACP were used as the primary material to be investigated. Analytical techniques such as X-ray microspectral (microprobe) analysis; scanning electron microscopy (SEM); and Raman structural analysis, including spatial mapping with a 2 μm step to diagnose the volumetric (3D) ratio of mineral phases in inclusion aggregates, were performed in all samples.

To prepare the samples, we polished both thin sections of ore minerals and resin-mounted ore minerals and analyzed them in transmitted and reflected light, respectively, by using a petrographic microscope (Olympus BX51) connected to an HD camera. In addition, the epoxy-mounted samples helped determine rock textures and mineral assemblages via SEM–energy-dispersive X-ray spectroscopy (EDS) with backscatter imaging analysis by using a TESCAN MIRA 3 LMU JSM-6510LV coupled with an X-Max EDS detector by Oxford Instruments.

We determined mineral composition by using an electron microprobe JEOL JXA-8100 (WDS mode, 20 kV, 15 nA, 1–2 μm beam diameter, manufacturer or laboratory, city, country). The accumulation time for fluorine (F) analysis (by using LDE crystal) was 40 s (20 s: counting of background; 20 s: counting peak for F); the F detection limit was 477 ppm (0.04 wt.%). For every mineral analysis run, we used a beam current of 10 nA and an acceleration voltage of 15 kV; except for Fe-Ti oxides: 20 nA and 15 kV, for monazite: 40 nA and 20 kV, for apatite: 10 nA and 20 kV. The peak counting time was 16 s for major elements and 30–60 s for minor elements. Calibration was carried out by using as standards both natural and synthetic phases (element, detection limits in ppm): SiO_2 (Si, 158); rutile (Ti, 120); $LiNbO_3$ (Nb, 142); Sr silicate glass (Sr, 442); albite (Na, 176); orthoclase (K, 182); Al_2O_3 (Al, 128); F-apatite (Ca, 115; P, 387; F, 477); Mn-garnet (Mn, 129); hematite (Fe, 148); $CePO_4$ (Ce, 236); $LaPO_4$ (La, 272); $BaSO_4$ (S, 178); $NdPO_4$ (Nd, 362); Cl-apatite (Cl, 74); and $PrPO_4$ (Pr, 401).

Raman spectroscopy was used to determine the composition of mineral phases in melt and fluid inclusions by using a LabRam HR800 Horiba Jobin Yvon spectrometer, which was equipped with an optical microscope (Olympus BX41, Olympus Corp., Tokyo, Japan). The 514.5 nm Ar+ laser line was used for spectra excitation. The well-known

RRUFF (http://rruff.info) database for Raman spectra was consulted to identify trapped solid phases. In addition, 2D mapping was carried out in several samples by using a Raman spectrometer with automatic confocal Raman imaging WITec Apyron. A 488 nm laser (50 mW) was applied to excite the sample. Phase separation and mapping were performed by using the "True component analysis" algorithm of the WITec Project FIVE+ software. The baseline, cosmic peaks, and, partly, the lines of neighboring phases were subtracted from the spectra.

Heating and cooling experiments on fluid inclusions were conducted by using a heat chamber TC-1500 with an inert atmosphere of purified argon and a Linkam THMSG-600 thermal stage. The experiments included the determination of homogenization temperatures and of the composition of salts and gases. Temperature data were also used to determine the concentrations of Na and K as an internal standard for the calculation of other element concentrations in the inclusions from Linkam LA-ICP-MS results.

All analytical methods were carried out at the Analytical Center for multi-elemental and isotope research Siberian Branch Russian Academy of Science (Novosibirsk, Russia).

The concentration of ore elements (Fe, Th, U, REE, etc.) and major cations (Ca, Mg, Rb, Sr, Cs, etc.) in discrete fluid inclusions was determined by using LA-ICP MS [37]. The set-up consisted of a Thermo-Scientific quadrupole inductively coupled plasma mass spectrometer XSERIES2. The mass spectrometer is integrated with a laser sampling device (New Wave Research), Nd: YAG solid-state laser. The certified standard NIST-612 was used for element calibration. In order to account for the matrix effect and sensitivity drift of the instrument, an internal standard was used. The majority of the inclusions that were investigated had representative sizes of approximately 20–50 μm. The arrangement that was used for the LA-ICP-MS analysis and the calculation of element concentrations in brine–melt inclusions in carbonatites of the Central Tuva region is described in [37]. The concentrations of Na, K, Ca, or Na, which were calculated according to microthermometric data (NaCl and KCl concentrations), as well as volumetric contents and SEM-EPMA analyses of daughter-phase inclusions (carbonates and sulfates), were used as internal standards to calculate element concentrations in the inclusions. Conversely, to obtain the composition of a single inclusion, the average value of the analytic signal of each element recorded during the ablation of the host mineral was subtracted from that obtained during the ablation of the fluid inclusion. Moreover, element concentrations in fluid inclusions were calculated by using an algorithm that was based on the formula of H. Longerich during LA-ICP MS analysis [58]. A similar calculation has been used in several publications on LA-ICP MS analysis of fluid inclusions [59,60]. The LA-ICP MS investigations were carried out at Novosibirsk State University (Novosibirsk, Russia).

4. Results

Microthermometry and Microanalysis of Fluid Inclusions

The first-ever-investigated crystal–fluid inclusions in *the Western Transbaikalia region* were collected from Yuznoe and Arshan REE-carbonatites [40]. It was revealed that bastnäsite-(Ce) in these carbonatites was formed at temperatures above 520°C. Additionally, the presence of salt daughter phases in the inclusions, comprising Na, K, and Ca sulfates, as well as fluorine-bearing minerals, was established. The formation temperature of fluorite at the Arshan and Yuzhnoe deposits was estimated to be within the range of 370–400°C [40]. The obtained data on fluorite mineralization are consistent with and complement our most recent research on the role of fluid regimes in the formation of fluorites from the Yuzhnoe and Arshan carbonatite complexes. In this research, we identified crystal–fluid (or brine–melt) inclusions with a concentration of 55-68 wt. %, containing predominantly Na-Ca-Sr sulfates and Na-Ca carbonates with homogenization temperatures of approximately 420–560 °C [41]. In this study, we present new results on optical and inclusion analyses of the composition of the phases that are embodied, as well as an overview of the formation conditions of melt and fluid inclusions in carbonatites and the

associated alkaline igneous rocks from the following Western Transbaikalia complexes: Khalyuta, Arshan, Yuzhnoe, and Ulan-Ude (Portovoe).

Modern advances in the interpretation of primary and primary–secondary melt inclusions in shonkinites and alkaline syenites of the Khalyuta complex have demonstrated the presence of two main types of inclusions: silicate and sulfate–carbonate–silicate (Figure 2a–h). The titanite in shonkinite contains inclusions of clinopyroxene, melt with crystals of K-feldspar, and phlogopite, as well as carbonate–sulfate–silicate inclusions with crystalline phases of anhydrite, calcite, baryto-celestine, K-feldspar, phlogopite, and Mss (monosulfide solid solution) (Figure 2a–d). K-feldspar in alkaline syenites also encloses sulfate–silicate inclusions with albite and baryte-celestine (Figure 2e). Further analysis of the composition of carbonate–sulfate–silicate inclusions in clinopyroxene from shonkinites revealed the presence of daughter phases of phlogopite, calcite, and anhydrite, as well as gaseous CO_2 (Figure 2g). Thermometric experiments on the same type of inclusions from the Khalyuta complex demonstrated signs of silicate–salt immiscibility at temperatures above 780–800 °C (Figure 2h), which is consistent with our previous report [46]. Detailed information on parameters associated with the entrapment of inclusions in minerals from carbonatites and associated magmatic rocks from Siberia and Mongolia may be found in the Supplementary Materials (Tables S1 and S3.1).

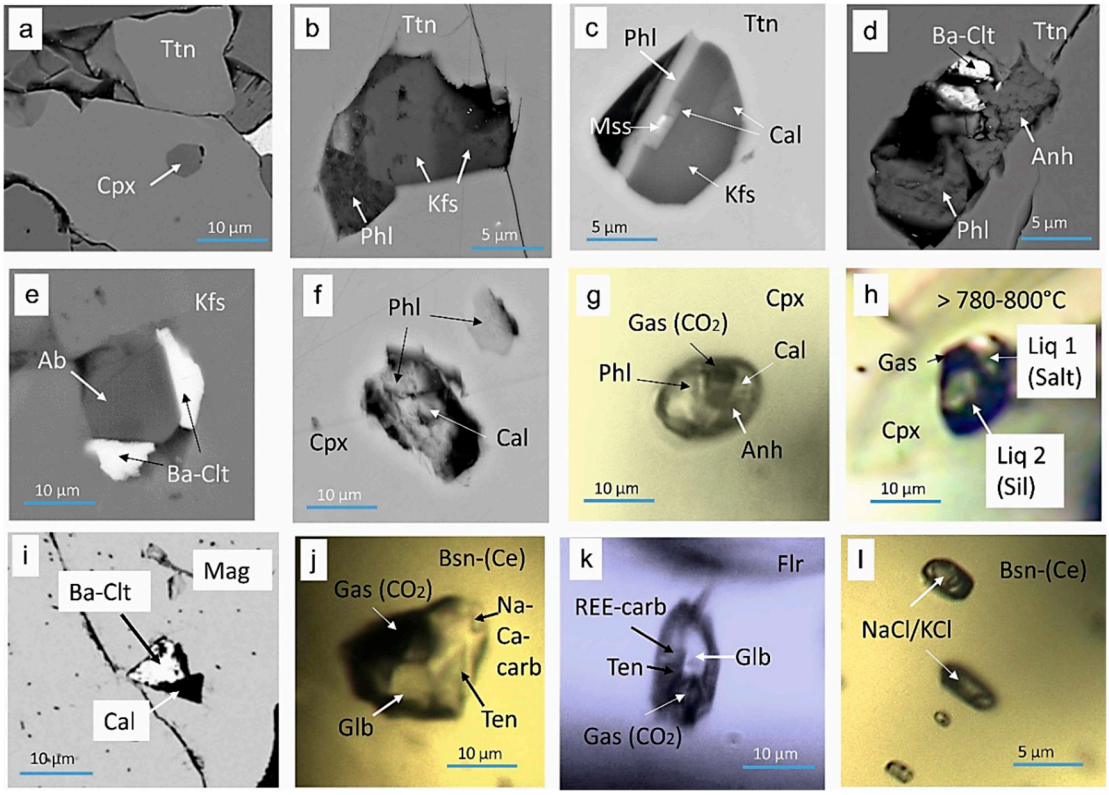

Figure 2. General aspects of inclusions in different minerals comprising carbonatites and associated alkaline magmatic rocks of the Western Transbaikalia carbonatite complexes. (**a**–**d**) Mineral, melt–silicate, and carbonate–sulfate–silicate inclusions in titanite from shonkinites; (**e**) sulfate–silicate inclusions in K-feldspar from alkaline syenites; (**f**) carbonate–sulfate–silicate inclusions in clinopyroxene from shonkinites of the Khalyuta complex (results from SEM-EPMA analysis). (**g**) Microphotographs of a melt inclusion, including the (**h**) results of thermometric studies of melt inclusions in shonkinite clinopyroxene (Khalyuta); (**i**) SEM-BSE image of a polymineral inclusion in magnetite from the Yuzhnoe carbonatite; (**j**) microphotograph of brine–melt inclusions in bastnaesite-(Ce); (**k**) microphotograph of brine–melt inclusions in fluorite; and (**l**) microphotograph of gas–liquid inclusions in bastnaesite-(Ce) from Ulan-Ude carbonatites. The Raman spectra for the crystalline phases of brine–melt inclusions (**j**–**l**) present in [52]. Abbreviations of mineral phases according to [53].

Inclusions of zircon are situated in magnetite from the carbonatites of the Yuzhnoe occurrence, as well as polymineral inclusions of sulfate-carbonate composition containing daughter phases of calcite, strontianite, and alkaline (Na-Ca) carbonates, as well as sulfates of baryto-celestine composition (Figure 2i). Fluid inclusions in bastnaesite and fluorite of the Ulan-Ude occurrence were derived from an orthomagmatic carbonatite saline melt, consisting of up to 90 vol.% salts, of carbonate (Ca, REE)–sulfate (Ca, Na) composition, at temperatures above 490–520°C [52]. Additionally, the analysis of daughter crystalline phases in brine–melt inclusions in bastnaesite and fluorite, of the Ulan-Ude complex, showed the presence of Na and Ca sulfates, such as glauberite and thenardite, as well as Ca and F-REE-carbonates, such as calcite (with an admixture of 0.5–2.3 wt. % SrO) and parisite/synchysite (?) (Figure 2j, k). Therefore, the fluorite–bastnaesite rocks of Ulan-Ude may represent a specific ore-bearing orthomagmatic fraction, which has been well established in all carbonatite complexes of the Western Transbaikalia.

The relevance of sulfate in the formation of the West Transbaikalia carbonatites is well-established [54]. Primary brine–melt inclusions with high concentrations (52–74 wt. %) of Na, -K-, Ba-Sr-, and Ca-sulfates (predominantly), as well as alkaline (Na-K-Ca) carbonates and fluorine-bearing REE-carbonates (bastnaesite-(Ce)), are found in carbonatites from the Yuzhnoe (bastnaesite), Khaluta, Arshan (fluorites), and Ulan-Ude (bastnaesite, fluorite) complexes. The gas phase includes $CO_2 \pm N_2 \pm H_2$. The homogenization temperatures of inclusions are greater than 480-560°C. As the orthomagmatic (carbothermic) fluid evolves into the hydrothermal stage, the conditions of mineral formation change in the TX system. At 520–440°C, a chloride–carbonate–sulfate (63–52 wt. %) brine evolves into a chloride–sulfate–carbonate (K, Ca, Na, Sr, Ba)-CO_2 (42–38 wt. %) solution. This solution is later diluted by meteoric waters at 400-370 °C. At 250–135°C, a hydrous-carbonate–sulfate–chloride solution (16–15 wt. %) evolves into a bicarbonate–chloride (Ca, Mg, Fe^{3+}, Na, K)-$CO_2 \pm N_2 \pm H_2$ low-concentration (<< 15 wt. % NaCl-eq.) solution (see Table S1; Table S3.1). Estimates of pressure entrapment for the Western Transbaikalia brine–melts, based on the density of carbon dioxide (thermo-freezing data), show an interval between 280 and 310 MPa, followed by a decrease to 250 MPa and below during fluid evolution.

In our previous study [37], we investigated the *Carbonatites of the Central Tuva region.* In this study, we present new data in conjunction with the results of previous studies to improve and integrate them with modern analyses of inclusion composition and capture regimes (Table S1). This approach has significantly enhanced our understanding of the primary formation stage of ankerite–calcite carbonatites (Figure 3a–d). Our results from melt inclusions in apatite, phlogopite, and quartz suggest that the ankerite–calcite carbonatites (the first intrusive stage of carbonatites) in the Karasug alkaline complex formed from a silicate–carbonate melt at temperatures above 790–820°C [37]. Additionally, modern thermometric studies and systematic compositional analyses of mineral phases in melt inclusions have revealed clear processes of carbonate–silicate immiscibility (Figure 3a). The ankerite composition contains an admixture of up to 3.2 wt.% SrO, while the silicate phase yields Si, Al, Ca, Na, K, Fe, Mg, Ti, O, Cl, and OH (Table S1). Furthermore, we found that fluorites from the ankerite–calcite carbonatites of the Karasug and Ulatai–Choza complexes enclose brine–melt inclusions of Na-K-Ca-Mg-Fe-(Ba-Sr) fluoride–sulfate–carbonate–chloride composition (Figure 3b—d; Table S1). The homogenization temperatures of the brine–melts range between 610 and 650°C, and these melts were trapped at a minimum pressure of 340-350 MPa [37]. The second stage of Tuva Fe-F-REE (ore)-bearing siderite carbonatites is intimately associated with the formation of Na-K-Ca-Fe-Ba-Sr-REE fluoride–carbonate–sulfate–chloride brine–melts at temperatures of 580-640°C and a pressure of 290—350 MPa (Figure 3e,f; Table S1; Table S3.1) [37]. The next stage of fluid evolution is linked to high-salinity (60–40 wt.%) Na-K-Ca-Ba-Sr-REE fluoride–carbonate–sulfate–chloride solutions and salty (40–30 wt.%) sulfate–hydrous carbonate–chloride fluid ($CO_2 \pm N_2$) solutions. These solutions formed at temperatures ranging between 480–420°C and 380-300°C and at pressures of about 250-180 MPa. The latter fluids are predominantly

CO_2-chloride in composition and are estimated to have formed at 300—250°C and 75–500 MPa (Table S1; Table S3.1) [37].

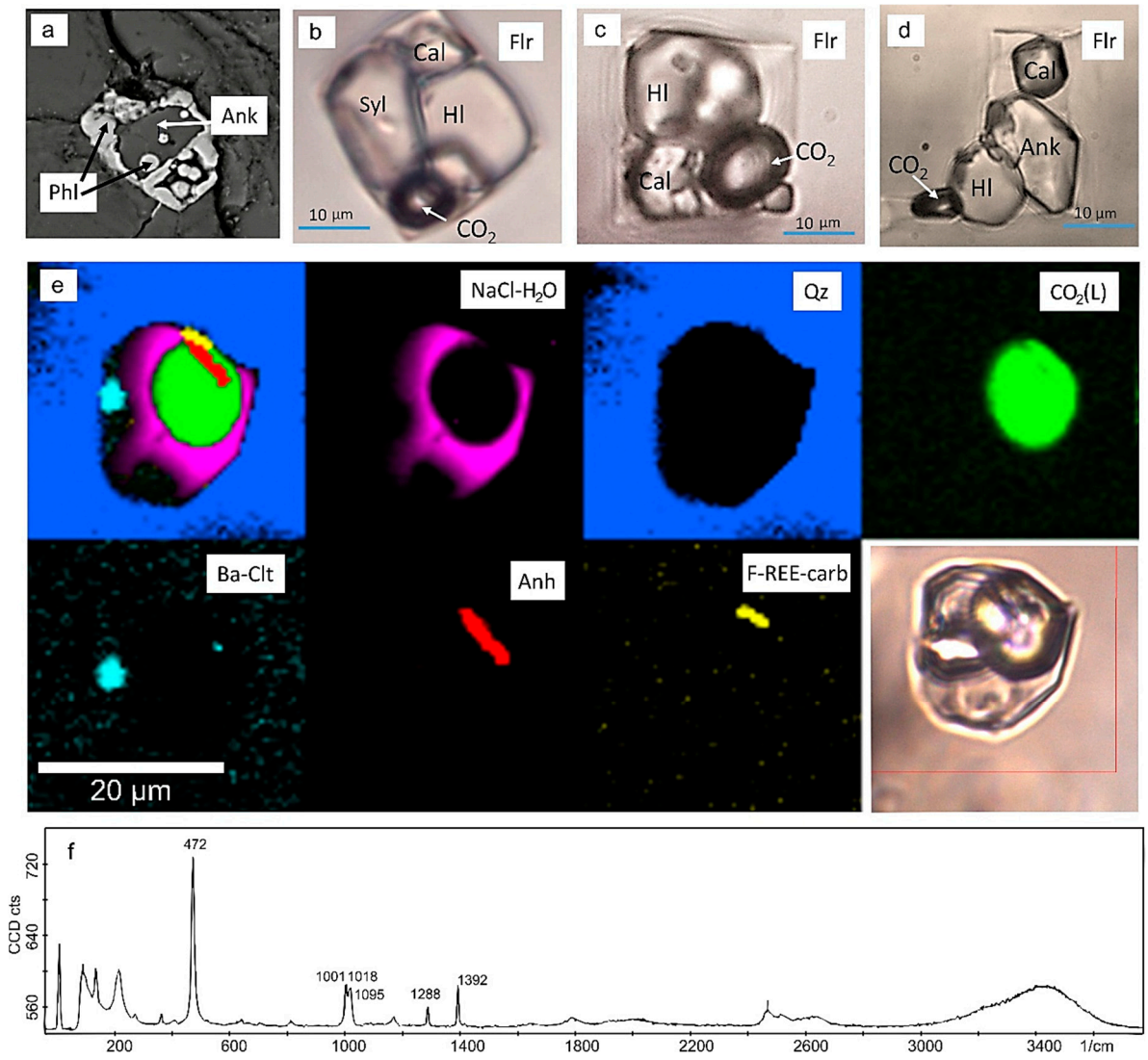

Figure 3. The composition of melt inclusions in carbonatites from the Central Tuva Region of Southern Siberia. Backscattered electron (BSE) image of an exposed melt inclusion (**a**), as well as microphotographs of brine–melt inclusions (**b**–**d**) in fluorite of ankerite–calcite carbonatites. Raman spectroscopy (**e**,**f**) showing the compositional mapping of a brine–melt inclusion in quartz from the Fe-F-Ba-Sr-REE-bearing siderite carbonatites.

Some studies have revealed that fractional crystallization and liquid–salt immiscibility contribute to the formation of melt inclusions in the alkaline silicate rocks of *the Mushugai-Khudag complex* [55,56]. The rock-forming minerals in the area, including melanephelinite, leucite phonolite, shonkinite, theralite, quartz syenite, rhyolite, magnetite–apatite, and celestite–fluorite, were found to have crystallized from silicate, salt–silicate, and salt melts in the range of 850–1220 °C [55,56]. Brine–melts of carbonate–phosphate, phosphate–sulfate, fluorine–sulfate, and chloride–sulfate compositions are believed to be responsible for the genesis of carbonatites and ore-bearing magnetite–apatite rocks [55]. Furthermore, recent research confirms that apatite–magnetite rocks were formed through crystallization differentiation from a silicate–salt melt with a high concentration of phosphates and sulfates at temperatures exceeding 830—850°C and pressures of 320–340 MPa [39]. To examine the type of fluid involved in carbonatite formation, we used our own database from previous work [39,57] and expanded the information

(Figure 4; Table S1) by analyzing melt inclusions in fluorapatite and fluorite from calcite–fluorite and apatite–magnetite rocks by using LA-ICP MS results.

Inclusions of melt and brine–melt in fluorapatite from magnetite–apatite rocks exhibit high concentrations (89–97 wt.%) of silicate and silicate–phosphate–sulfate–CO_2(L) fluids, which homogenize at 830–850°C and 500—580°C, respectively (Figure 4a-e; Table S1). Crystal–fluid inclusions in apatite also contain phosphate–sulfate–chloride solutions (ranging from 60-45 to 20-10 wt.%) with homogenization temperatures falling within two ranges: 480—380 and 250—150°C (Figure 4f; Table S1; Table S3.1). Meanwhile, brine–melt inclusions in fluorite from the calcite–fluorite rocks of the Mushugai-Khudag complex are composed of fluids with a carbonate–chloride–sulfate–CO_2(L) composition (52–64 wt.%), and they homogenize at temperatures ranging from 500 to 530°C (Figure 4j—I; Table S1). Late-stage quartz–carbonate–celestite–fluorite rocks were formed with the involvement of carbonate–sulfate–chloride–CO_2(L)/CO_2 ± H_2 dense solutions, which vary in concentration from 46-38 to 13.9—6.5 wt. % and in homogenization ranging from 470–390°C to 295–250 °C (Figure 4 k; Table S1; Table S3.1).

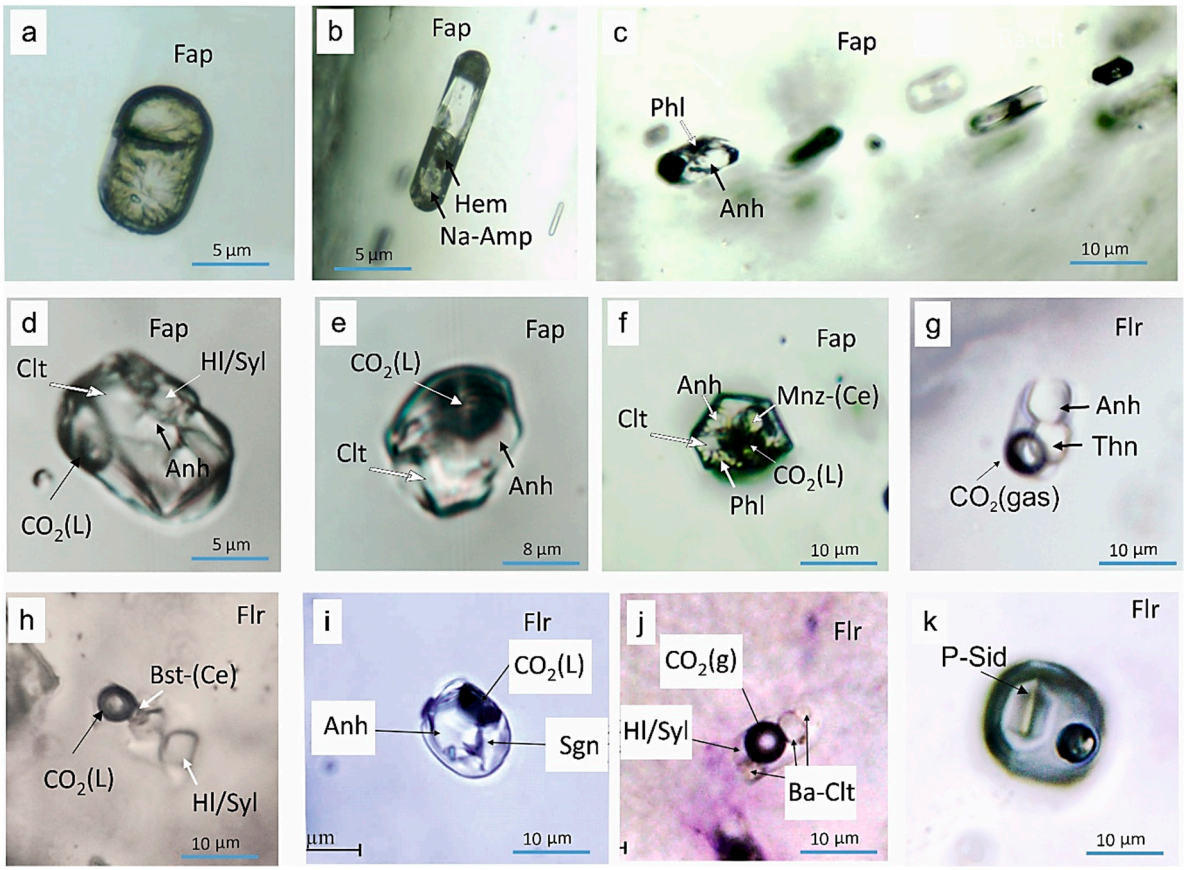

Figure 4. Melt inclusions of the Mushugai-Khudag alkaline complex, including melt of Ca-P-K-Na-silicate composition (**a**) and silicate–phosphate–sulfate–CO_2(L) brine–melt (**b**–**f**) inclusions, as well as crystal–fluid inclusions in fluorapatite from the magnetite–apatite rocks. (**g**–**k**) The brine–melt of carbonate–chloride–sulfate–CO_2(L) composition and inclusions of crystal–fluid carbonate-sulfate-chloride-CO_2±H_2 in fluorite from the calcite–fluorite rocks are also shown, along with crystal–fluid inclusions in fluorite from late-stage quartz–carbonate–celestite-fluorite rocks.

A study was conducted to investigate the metal-bearing capacity of carbonatite brine–melts by using LA-ICP MS. The objective of the study was to analyze individual fluid inclusions in quartz and fluorite from carbonatites in Southern and Eastern Siberia, as well as from the Mushugai-Khudag complex, which includes both carbonatites and magnetite–apatite rocks (Table S2; Table S3.2; Table S3.3; Table S3.4).

The results of the study show that alkaline rocks from the Central Asian carbonatite province exhibit high concentrations of Na, K, Fe, Mn, Ca, Sr, and Ba, of 0.5n–10n wt. %, and high LREE and Y, of approximately 10n ppm—0.1–1n wt. %. In addition, high concentrations of Th and U were observed, which ranged from 0.1n to 10 n ppm (Table S2; Table S3.2; Table S3.3; Table S3.4). Figure 5 displays different stack bars showing the relative element concentration for a given composition of the brine–melt inclusions.

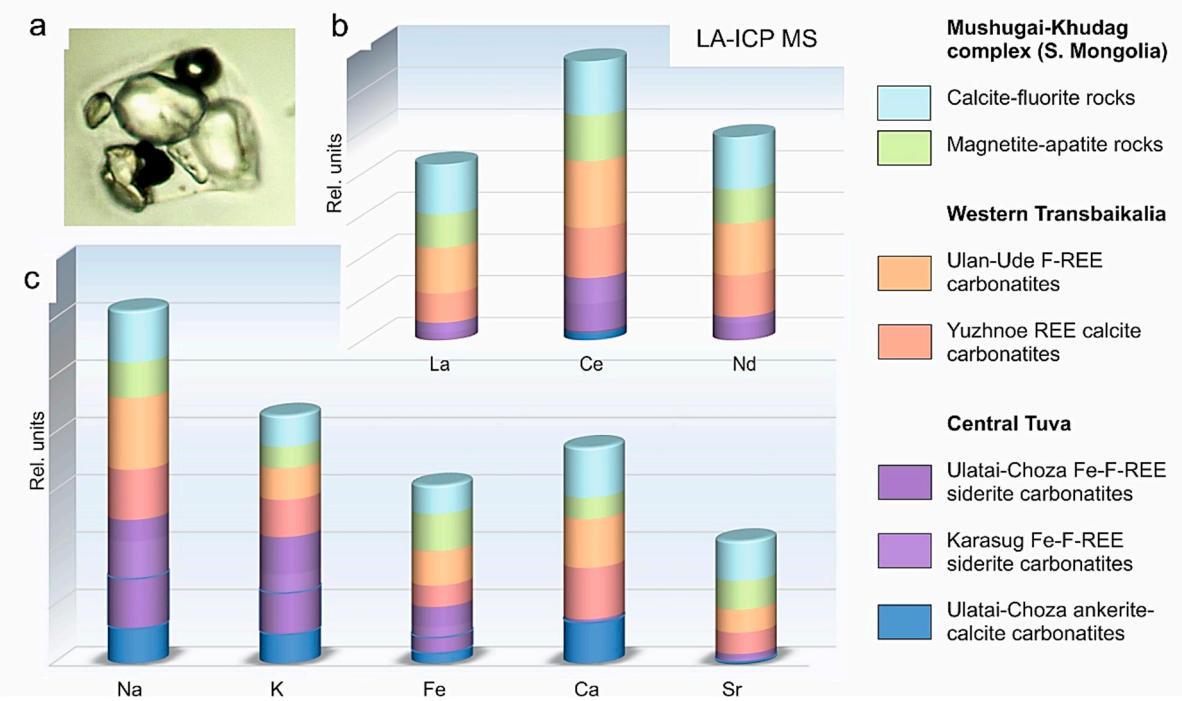

Figure 5. Results from LA-ICP-MS investigations on brine–melt inclusions in the alkaline complexes of the Central Asian carbonatite province. (**a**) Representative microphotograph of a brine–melt inclusion. (**b**,**c**) Stacked bars of relative element concentration in brine–melt inclusions of different origins.

Our LA-ICP-MS data reveal that carbonatites of the Central Tuva region have relatively high concentrations of Na and K, similar to the Yuzhnoe carbonatites from Western Transbaikalia (Figure 5). On the other hand, higher Ca contents in brine–melt inclusions are more typical of calcite carbonatites from Tuva and Transbaikalia and of fluorite-bearing rocks from Mushugai-Khudag. Additionally, Fe-ores are intrinsic to the magnetite–apatite rocks of Southern Mongolia, as well as the siderite carbonatites of Central Tuva (Figure 5b). Meanwhile, LREE (light rare earth elements) are evenly distributed in the brine–melts of REE-carbonatites of the Central Asian province. However, a slightly higher amount of Ce is characteristic of the carbonatite ores from the Ulan-Ude and Karasug deposit (Figure 5c).

5. Discussion

Petrogenetic Aspects of Carbonatites

Detailed analyses of melt and fluid inclusions in carbonatites and associated alkaline–silicate rocks from the Central Asian carbonatite province have revealed the participation of both silicate–salt immiscibility and fractional crystallization mechanisms in the origin of these carbonatite complexes. However, it is crucial to understand the specific stages and formation mechanisms of ore-bearing associations during the mantle–crustal evolution of the primary carbonatite fluid–melts. As mentioned previously in the Introduction, the immiscibility alone cannot account for the concentration of REEs in carbonatites [61,25]. Nevertheless, during the early stages of crystallization, agents such as F, S,

P, Cl, and calcite may participate in the accumulation of REEs [26]. When carbonatite melts become saturated with calcite and large amounts of carbonatite cumulates are formed, REEs become highly enriched in the liquid fraction due to their incompatibility with calcite [26]. Consequently, as carbonatite melts evolve into cumulates with higher Mg and Fe contents, key components (or agents) such as Na^+, K^+, Ca^{2+}, H_2O, CO_2, fluorides, chlorides, and sulfates remain in the melt, acting as fluxes. These volatile flows are particularly fixed in carbonatite minerals in the form of specific brine–melt inclusions [37,62,63]. Therefore, interpreting the entrapment conditions and mechanisms by which brine–melt inclusions develop into fluid ones can also provide insight into the assessment of ore-forming processes in carbonatite complexes via the obtained PTX parameters.

Our study on the carbonatite complexes of the Central Asian fold belt enabled us to identify the compositional features and physicochemical conditions under which the entrapment of melt, brine–melt, and fluid inclusions occurred. Based on this information, we developed a preliminary petrogenetic model of alkaline–carbonatite systems and assessed the mechanisms and conditions of (ore-) mineral formation (Table S1,S2, Figure 6). We observed a very similar fluid evolution path, from brine–melts to carbothermal and/or hydrothermal fluids, as well as comparable mineral and ore-forming processes for identical F-REE types of carbonatite complexes in various regions. These regions include the Central Taimyr region (Arctica) [64], the carbonatites of the Roman Region (Italy) [22,65], and well-known alkaline–carbonatite complexes such as Bayan Obo, Maoniuping, and Dalucao (China) [7,8], as well as carbonate-rich rocks of Amba Dongar in India [9], Kangankunde in Malawi [10], Okorusu in Namibia [11], and Barra do Itapirapuã in Brazil [12]. The results of these investigations may contribute to the understanding of mantle sources, but the mantle source composition is not presented in this report.

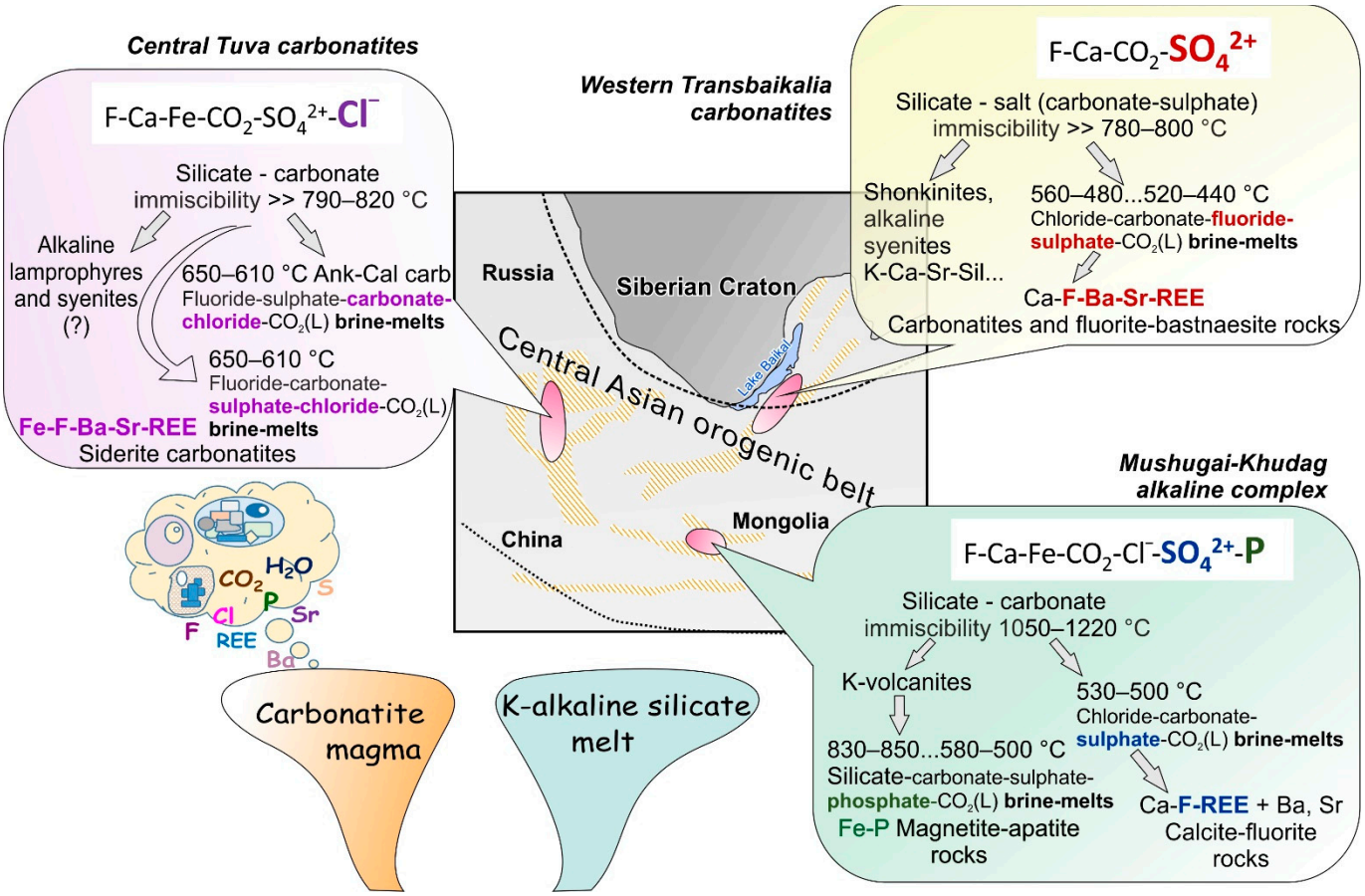

Figure 6. Petrogenetic model of alkaline carbonatite complexes from the Central Asian carbonatite province, depicting information on the composition of melt and brine–melt inclusions that are related to the formation of ore deposits.

The alkaline–carbonatite complexes of Western Transbaikalia are genetically associated with K-alkaline–silicate rocks such as shonkinites and alkaline syenites. Melt inclusion data indicate that the carbonatites of the Khalyuta complex formed due to silicate–carbonate–sulfate immiscibility at temperatures above 780–800 °C (Table S1; Figure 6). Brine–melts of the Khalyuta, Yuzhnoe, Arshan, and Ulan-Ude carbonatites have an alkaline chloride–carbonate–fluorine–sulfate composition and were formed at temperatures ranging from 560–480 to 520–440 °C at trapping pressures of approximately 280–310 MPa (Table S1; Figure 6). The main ore-bearing (F-Ba-Sr-REE) mineral assemblages were formed from brine–melts and can be found in calcite, fluorite, bastnaesite-(Ce), biotite, barite, celestite, monazite-(Ce), albite, K-feldspar, Nb-rutile, ilmenite, glauberite, plumbojarosite, etc. (Table S1). Notably, specific brine–melts are significantly enriched in ores, such as the fluorite–bastnaesite carbonatites of the Ulan-Ude complex, where the concentration of light lanthanides can reach up to a few percent, which distinguishes them from other deposits of the Central Asian province (Table S2 and Figure 5). The next stage of mineral formation and mineralization of barite, fluorite, calcite, celestite, monazite-(Ce), parisite-(Ce), synchysite-(Ce), siderite, etc., is related to concentrated fluids of sulfate–carbonate–chloride and bicarbonate–chloride compositions, with homogenization temperatures ranging between 400–370 °C and 250–135 °C and enclosing pressures below 250 MPa (Table S1).

The carbonatites in the Central Tuva region were emplaced in two stages, producing ankerite–calcite and siderite ore-bearing carbonatites, but their relationship with spatially associated alkaline silicate rocks in lamprophyres and alkaline syenite complexes has yet to be determined. However, our melt inclusions study on carbonatites clearly indicates evidence of silicate–carbonate immiscibility (>> 790–820 °C) (Table S1; Figure 6). The brine–melts of ankerite–calcite carbonatites in the Karasug and Ulatai-Choza complexes have a fluorite–sulfate–carbonate–chloride composition with homogenization temperatures of approximately 610–650 °C and trapping pressures above 350 MPa (Table S1; Figure 6). In the first stage of formation, the Central Tuva carbonatites crystallized calcite, ankerite, phlogopite, fluorapatite, Ti-magnetite, quartz, albite, muscovite, fluorite, monazite-(Ce), and bastnaesite-(Ce) (Table S1). The ore-bearing Fe-F-Ba-Sr-REE brine–melts of siderite carbonatites yield a fluorite–carbonate–sulfate–chloride composition, with homogenization temperatures of brine–melts of about 650–610 °C and enclosing pressures of 290-350 MPa (Table S1; Figure 6). This stage produced siderite, calcite, dolomite, fluorite, quartz, barite, Ba-celestite, bastnaesite-(Ce), fluorapatite, muscovite, and magnetite (Table S1). Moreover, the ore-bearing brine–melts of siderite carbonatites are enriched in high Ce and K (Figure 5). The hydrothermal stage of the Central Tuva carbonatites is related to saline fluoride–carbonate–sulfate–chloride and sulfate–hydrous-carbonate–chloride fluid solutions derived at 480–420 °C and 380–300 °C and pressures of approximately 250–180 MPa. These fluids were responsible for the second ore-forming stage in carbonatites, which include mineral assemblages with siderite, calcite, dolomite, fluorite, quartz, barite, Ba-celestite, bastnaesite-(Ce), parisite-(Ce), synshysite-(Ce), xenotime-(Y), fluorapatite, strontianite, and sericite (Table S1).

The Mushugai-Khudag alkaline complex is composed of various types of ore-bearing rocks, such as magnetite–apatite and calcite–REE–carbonate–celestine–fluorite, formed through silicate–salt (carbonate–sulfate) immiscibility, fractional crystallization, or immiscibility that generated a separate iron phosphate fraction from the brine–melts (Table S1; Figure 6). The experimental replication of the latter process has been reported [66]. The brine–melts mostly exhibit silicate–chloride–phosphate (in magnetite–apatite rocks) and carbonate–chloride–fluorine–sulfate (in REE–carbonate–fluorite rocks) compositions, with distinct homogenization temperature ranges of 830-850 °C and 500–580 °C (Table S1; Figure 6). On the other hand, silicate–chloride–phosphate brine–melts gave rise to the formation of magnetite, fluorapatite, ilmenite, and phlogopite, while fluorine–sulfate brine–melts led to the crystallization of magnetite, calcite, apatite, fluorite, barite, celestite, and REE carbonates and phosphates (Table S1; Figure 6). Additionally, crystal–fluid inclusions

composed of carbonate–chloride–sulfate with homogenization temperatures of 500–530 °C and hydrothermal carbonate–sulfate–chloride fluids with homogenization temperatures ranging from 470–390 °C to 295–250 °C are closely associated with ore-bearing mineralization of monazite-Ce, celestite, rutile, quartz, fluellite, fluorite, barite, gypsum, bastnaesite-(Ce), monazite-(Ce), ilmenite, rutile, siderite, and phosphosiderite (Table S1).

6. Conclusions

In this study, we conducted comprehensive investigations of the physicochemical parameters of melt and fluid inclusions in rock-forming minerals from alkaline rocks in the Central Asian carbonatite province. Our findings revealed that these minerals were formed through silicate–carbonate (salt) immiscibility processes, involving fractional crystallization. The alkaline–carbonatite cumulates correspond to distinct saline–melt fractions that differ in the amount of main salt components, thus defining the type and concentration of ores. These salt fractions are unambiguously identified as brine–melt inclusions, which are directly linked to the processes of orthomagmatic carbonatite mineralization, as well as the first stage of ore formation.

In addition, our results demonstrate that the brine–melts are responsible for the F-Ba-Sr-REE mineralization in carbonatites and that their compositions differ depending on the type of carbonatite. In the *Western Transbaikalia* carbonatites, the brine–melts have an alkaline chloride–carbonate–fluorine–sulfate composition, and their formation is associated with temperatures of approximately 560–440 °C and pressures of 280–310 MPa. The ankerite–calcite carbonatites of the *Central Tuva* complexes have brine–melts with a fluorite–sulfate–carbonate–chloride composition, which is characterized by homogenization temperatures of approximately 610–650 °C and trapping pressures above 350 MPa.

In the siderite carbonatites, the ore-bearing brine–melts correspond mainly to fluorite–carbonate–sulfate–chloride compositions, with homogenization temperatures of approximately 650–610 °C and enclosing pressures ranging from 290 to 350 MPa. In the *Mushugai-Khudag* complex, the brine–melts of alkaline ore-bearing rocks have a silicate–chloride–phosphate composition, while magnetite–apatite rocks are characterized by carbonate–chloride–fluorine–sulfate composition, including REE–carbonate–fluorite rocks. Homogenization temperatures for the brine–melts were observed to be 830–850 °C and 500–580 °C.

The final stages of carbonatite system evolution, which include the formation of ore deposits, are closely linked to the presence of saline hydrothermal fluids, as evidenced by the presence of saline crystal–fluid inclusions. These fluids are believed to be responsible for the second stage of F-(Ba)-(Sr)-REE mineralization. In the CACP complexes, the saline crystal–fluid inclusions typically exhibit fluorine–sulfate–carbonate–chloride and bicarbonate–chloride compositions, with homogenization temperatures ranging from 480 to 250 °C and trapping pressures below 250 MPa.

The evolution of carbonatite systems from brine–melts to purely hydrothermal fluids, as well as the ore and mineral formation processes described here, may represent natural mechanisms that are applicable to other F-REE carbonatite complexes, whether they are associated with rift-related plumes or occur in orogenic belts.

Overall, this study provides insight into the diverse nature of brine–melts in carbonatite complexes and their role in the process of mineralization. The results can be useful for understanding the mechanisms underlying the formation of ore deposits in these rocks.

Supplementary Materials: The following supporting information can be downloaded at: https://www.mdpi.com/article/10.3390/min13040573/s1, Table S1: melt and fluid inclusion data of carbonatite complexes of the Central Asian province (Russian Siberia and South Mongolia), Table S2: LA-ICP MS elemental concentrations in the brine-melt inclusions in the carbonatites of the Central Asian province, Table S3.1: thermometric inclusion data, Table S3.2: LA-ICP MS results for Ulatai-Choza (Tuva) inclusions in siderite carbonatite (quartz), Table S3.3: LA-ICP MS results for

Western Transbaikalia inclusions in carbonatites (fluorite), Table S3.4: LA-ICP MS results for Mushugai-Khudak (Mongolia) inclusions (fluorapatite, fluorite).

Author Contributions: Conceptualization, I.P.; methodology, I.P., A.D. and A.R.; field research and sample collection, I.P., A.D. and A.R.; data curation and validation, I.P and A.D.; laboratory research, I.P., A.D. and A.R.; writing of original draft, I.P.; writing—review and editing, I.P., A.D. and A.R. All authors have read and agreed to the published version of the manuscript.

Data Availability Statement: The data that support the findings of this study are available from the corresponding author upon reasonable request.

Funding: Melt and fluid inclusion studies were supported by the Russian Science Foundation Grant No. 22-17-00078 (https://rscf.ru/en/project/22-17-00078/). Geological investigation is done on state assignment of IGM SB RAS (122041400241-5) and GIN SB RAS (AAAA-A21-121011390002-2). Field work of carbonatites from the Central Tuva region was executed under TuvIKOPR SB RAS state contract No. 121031500140-2.

Acknowledgments: The authors express their sincere appreciation to the editor and reviewers for their contributions to improving the manuscript. All analytical methods were carried out at the Analytical Center for multi-elemental and isotope research Siberian Branch Russian Academy of Science and the Novosibirsk State University (Novosibirsk, Russia).

Conflicts of Interest: The authors declare no conflicts of interest.

References

1. Berger, V.I.; Singer, D.A.; Orris, G.J. Carbonatites of the world, explored deposits of Nb and REE; database and grade and tonnage models. *U.S. Geol. Surv. Open-File Rep.* **2009**, *1139*, 17.
2. Chakhmouradian, A.R.; Wall, F. Rare Earth Elements: Minerals, Mines, Magnets (and More). *Elements* **2012**, *8*, 333–340. https://doi.org/10.2113/gselements.8.5.333.
3. Nassar, N.T.; Du, X.; Graedel, T.E. Criticality of the Rare Earth Elements. *J. Ind. Ecol*. **2015**, *19*, 1044–1054.
4. Verplank, P.L.; Mariano, A.N.; Mariano, A., Jr. Rare earth element ore geology of carbonatites. *Soc. Econ. Geol*. **2016**, *18*, 5–32.
5. Wang, Z.-Y.; Fan, H.-R.; Zhou, L.; Yang, K.-F.; She, H.-D. Carbonatite-Related REE Deposits: An Overview. *Minerals* **2020**, *10*, 965. https://doi.org/10.3390/min10110965.
6. Anenburg, M.; Broom-Fendley, S.; Chen, W. Formation of Rare Earth Deposits in Carbonatites. *Elements* **2021**, *17*, 327–332. https://doi.org/10.2138/gselements.17.5.327.
7. Fan, H.-R.; Yang, K.-F.; Hu, F.-F.; Liu, S.; Wang, K.-Y. The giant Bayan Obo REE–Nb–Fe deposit, China: Controversy and ore genesis. *Geosci. Front*. **2016**, *7*, 335–344. https://doi.org/10.1016/j.gsf.2015.11.005.
8. Zheng, X.; Liu, Y. Mechanisms of element precipitation in carbonatite-related rare-earth element deposits: Evidence from fluid inclusions in the Maoniuping deposit, Sichuan Province, southwestern China. *Ore Geol. Rev*. **2019**, *107*, 218–238.
9. Dhote, P.; Bhan, U.; Verma, D. Genetic model of carbonatite hosted rare earth elements mineralization from Ambadongar Carbonatite Complex, Deccan Volcanic Province, India. *Ore Geol. Rev.* **2021**, *135*, 104215. https://doi.org/10.1016/j.oregeorev.2021.104215.
10. Chikanda, F.; Tsubasa, O.; Ohtomo, Y.; Ito, A.; Yokoyama, TD.; Sato, T. Magmatic-Hydrothermal Processes Associated with Rare Earth Element Enrichment in the Kangankunde Carbonatite Complex, Malawi. *Minerals* **2019**, *9*, 442. https://doi.org/10.3390/min9070442.
11. Cangelosi, D.; Broom-Fendley, S.; Banks, D.; Morgan, D.; Yardley, B. Light rare earth element redistribution during hydrothermal alteration at the Okorusu carbonatite complex, Namibia. *Mineral. Mag*. **2020**, *84*, 49–64. https://doi.org/10.1180/mg.m.2019.54.
12. Ruberti, E.; Enrich, G.E.R.; Gomes, C.B.; Comin-Chiaramonti, P. Hydrothermal REE fluorocarbonate mineralization at Barra do Itapirapuã, a multiple stockwork carbonate, southern Brazil. *Can. Mineral*. **2008**, *46*, 901–914.
13. Wallace, M.E.; Green, D.H. An experimental determination of primary carbonatite magma composition. *Nature* **1988**, *335*, 6188, 343–346.
14. Dalton, J.A.; Wood, B.J. The compositions of primary carbonate melts and their evolution through wallrock reaction in the mantle. *Earth Planet. Sci. Lett*. **1993**, *119*, 511–525.
15. Wyllie, P.J.; Lee, W.J. Model system controls on conditions for formation of magnesiocarbonatite and calciocarbonatite magmas. *J. Petrol*. **1998**, *39*, 1885–1893.
16. Gittins, J. The origin and evolution of carbonatite magmas. In *Carbonatites: Genesis and Evolution*; Unwin-Hyman: London, UK, 1989; pp. 580–600.
17. Gittins, J.; Jago, B.C. Differentiation of natrocarbonatite magma at Oldoinyo Lengai volcano, Tanzania. *Mineral Mag*. **1998**, *62*, 759–768.

18. Kjarsgaard, B.A.; Hamilton, D.L. The genesis of carbonatites by immiscibility. In *Carbonatites: Genesis and Evolution*; Unwin-Hyman: London, UK, 1989; pp. 388–404.
19. Lee, W.; Wyllie, P.J. Liquid immiscibility in the join $NaAlSiO_4$-$NaAlSi_3O_8$-$CaCO_3$ at 1 GPa: Implications for crystal carbonatites. *J. Petrol*. **1997**, *38*, 1113–1135.
20. Koster van Groos, A.F.; and P. J. Wyllie. Liquid immiscibility in the system Na_2O-Al_2O_3-SiO_2-CO_2 at pressures to 1 kilobar. *Am. J. Sci.* **1996**, *264*, 234–255.
21. Rankin, A.; Le Bas, M. Liquid immiscibility between silicate and carbonate melts in naturally occuring ijolite magma. *Nature* **1974**, *250*, 206–209. https://doi.org/10.1038/250206a0.
22. Stoppa, F.; Woolley, A.R. The Italian carbonatites: Field occurrence, petrology and regional significance. *Mineral. Petrol.* **1997**, *59*, 43–67. https://doi.org/10.1007/BF01163061.
23. Mitchell, R.H.; Dawson, J.B. Carbonate–silicate immiscibility and extremelyperalkaline silicate glasses from Nasira cone and recent eruptions at Oldoinyo Lengai Volcano, Tanzania. *Lithos* **2012**, *152*, 40–46. https://doi.org/10.1016/j.lithos.2012.01.006.
24. Solovova, I.P.;Girnis, A.V. Silicate–carbonate liquid immiscibility and crystallization of carbonate and K-rich basaltic magma: Insights from melt and fluid inclusions. *Mineral. Mag.* **2012**, *76*, 411.
25. Veksler, I.V.; Dorfman, A.M.; Dulski, P.; Kamenetsky, V.; Danyushevsky, L.; Jeffries, T.; Dingwell, D.B. Partitioning of elements between silicate melt and immiscible fluoride, chloride, carbonate, phosphate and sulfate melts, with implications to the origin of natrocarbonatite. *Geochim. Cosmochim. Acta* **2012**, *79*, 20–40. https://doi.org/10.1016/j.gca.2011.11.035.
26. Chebotarev, D.A.; Wohlgemuth-Ueberwasser, C.; Hou, T. Partitioning of REE between calcite and carbonatitic melt containing P, S, Si at 650–900 °C and 100 MPa. *Sci. Rep.* **2022**, *12*, 3320. https://doi.org/10.1038/s41598-022-07330-0.
27. Hou, T.; Charlier, B.; Holtz, F.; Veksler, I.; Zhang, Z.; Thomas, R.; Namur, O. Immiscible hydrous Fe–Ca–P melt and the origin of iron oxide-apatite ore deposits. *Nat. Commun.* **2018**, *9*, 1415. https://doi.org/10.1038/s41467-018-03761-4.
28. Mitchell, R.H. Carbonatites and carbonatites and carbonatites. *Can. Mineral.* **2005**, *43*, 2049.
29. Elliott, H.A.L.; Wall, F.; Chakhmouradian, A.R.; Siegfried, P.R.; Dahlgren, S.; Weatherley, S.; Finch, A.A.; Marks, M.A.W.; Dowman, E.; Deady, E. Fenites associated with carbonatite complexes: A review. *Ore Geol. Rev.* **2018**, *93*, 38–59. https://doi.org/10.1016/j.oregeorev.2017.12.003.
30. Walter, B.F.; Giebel, J.R.; Steele-MacInnis, M.; Marks, M.A.W.; Kolb, J.; Markl, G. Fluids associated with carbonatitic magmatism: A critical review and implications for carbonatite magma ascent. *Earth-Sci. Rev.* **2021**, *215*, 103509. https://doi.org/10.1016/j.earscirev.2021.103509.
31. Harlov, D.E.; Förster, H.-J.; Nijland, T.G. Fluid-induced nucleation of (Y + REE)-phosphate minerals within apatite: Nature and experiment. Part I. Chlorapatite. *Am. Mineral.* **2002**, *87*, 245–261. https://doi.org/10.2138/am-2002-2-306.
32. Williams-Jones, A.E.; Migdisov, A.A.; Samson, I.M. Hydrothermal Mobilisation of the Rare Earth Elements—A Tale of 'Ceria' and 'Yttria'. *Elements* **2012**, *8*, 355–360. https://doi.org/10.2113/gselements.8.5.355.
33. Tropper, P.; Manning, C.E.; Harlov, D.E. Solubility of $CePO_4$ monazite and YPO_4 xenotime in H_2O and H_2O–NaCl at 800 °C and 1GPa: Implications for REE and Y transport during high-grade metamorphism. *Chem. Geol.* **2011**, *282*, 58–66. https://doi.org/10.1016/j.chemgeo.2011.01.009.
34. Broom-Fendley, S.; Styles, M.T.; Appleton, J.D.; Gunn, G.; Wall, F. Evidence for dissolution-reprecipitation of apatite and preferential LREE mobility in carbonatite-derived late-stage hydrothermal processes. *Am. Mineral.* **2016**, *101*, 596–611. https://doi.org/10.2138/am-2016-5502CCBY.
35. Chakhmouradian, A.R.; Reguir, E.P.; Zaitsev, A.N.; Couëslan, C.; Xu, C.; Kynický, J.; Mumin, A.H.; Yang, P. Apatite in carbonatitic rocks: Compositional variation, zoning, element partitioning and petrogenetic significance. *Lithos* **2017**, *274–275*, 188–213. https://doi.org/10.1016/j.lithos.2016.12.037.
36. Prokopyev, I.R.; Doroshkevich, A.G.; Ponomarchuk, A.V.; Sergeev, S.A. Mineralogy, age and genesis of apatite-dolomite ores at the Seligdar apatite deposit (Central Aldan, Russia). *Ore Geol. Rev.* **2017**, *81*, 296–308. https://doi.org/10.1016/j.oregeorev.2016.10.01220.
37. Prokopyev, I.R.; Borisenko, A.S.; Borovikov, A.A.; Pavlova, G.G. Origin of REE-rich ferrocarbonatites in southern Siberia (Russia): Implications based on melt and fluid inclusions. *Mineral. Petrol.* **2016**, *110*, 845–859. https://doi.org/10.1007/s00710-016-0449-z.
38. Song, W.; Xu, C.; Veksler, I.V.; Kynicky, J. Experimental study of REE, Ba, Sr, Mo and W partitioning between carbonatitic melt and aqueous fluid with implications for rare metal mineralization. *Contrib. Mineral. Petrol.* **2016**, *171*, 1. https://doi.org/10.1007/s00410-015-1217-5I.R.
39. Nikolenko, A.M.; Redina, A.A.; Doroshkevich, A.G.; Prokopyev, I.R.; Ragozin, A.L.; Vladykin, N.V. The origin of magnetite-apatite rocks of Mushgai-Khudag Complex, South Mongolia: Mineral chemistry and studies of melt and fluid inclusions. *Lithos* **2018**, *320–321*, 567–582. https://doi.org/10.1016/j.lithos.2018.08.030.
40. Doroshkevich, A.G.; Ripp, G.S. Estimation of the conditions of formation of REE-carbonatites in Western Transbaikalia. *Russ. Geol. Geophys.* **2004**, *45*, 492–500.
41. Redina, A.A.; Doroshkevich, A.G.; Veksler, I.V.; Wohlgemuth-Ueberwasser, C.C. Fluorite Mineralization Related to Carbonatitic Magmatism in the Western Transbaikalia: Insights from Fluid Inclusions and Trace Element Composition. *Minerals* **2021**, *11*, 1183. https://doi.org/10.3390/min11111183.
42. Doroshkevich, A.G.; Kobylkina O.V.: Ripp, G.S. Role of sulfates in the formation of carbonatites in the Western Transbaikal region. *Dokl. Earth Scien.* **2003**, *388*, 131–134 (in Russian).

43. Nikiforov, A.V.; Yarmolyuk, V.V. Late Mesozoic carbonatite provinces in Central Asia: Their compositions, sources and genetic settings. *Gondwana Res. Vol*. **2019**, *69*, 56–72.
44. Vladykin, N.V. Potassium alkaline lamproite-carbonatite complexes: Petrology, genesis, and ore reserves. *Russ. Geol. Geophys*. **2009**, *50*, 1119–1128. https://doi.org/10.1016/j.rgg.2009.11.010.
45. Ripp, G.S.; Kobylkina, O.V.; Doroshkevich, A.G.; Sharakshinov, A.O. *Late Mesozoic Carbonatites of the Western Transbaikalia*. Izd-vo BNTs SO RAN: Ulan-Ude, Russia, 2000: 95 p. (In Russian)
46. Doroshkevich, A.G.; Ripp, G.S.; Moore, K.R. Genesis of the Khaluta alkaline-basic Ba-Sr carbonatite complex (West Transbaikala, Russia). *Mineral. Petrol.* **2010**, *98*, 245–268.
47. Doroshkevich, A.G.; Ripp, G.S.; Viladkar, S.G.; Vladykin, N.V. The Arshan REE carbonatites, southwestern Transbaikalia: Mineralogy, paragenesis and evolution. *Can. Mineral.* **2008**, *46*, 807–823.
48. Nikiforov, A.V.; Bolonin, A.V.; Lychin, D.A.; Sugorakova, A.M.; Popov, V.A. Carbonatites of central Tuva: Geological structure and min-eral and chemical composition. *Geol. Ore Depos.* **2005**, *47*, 326–345. (In Russian)
49. Samoilov, V.S.; Kovalenko, V.I. *Complexes of Alkaline Rocks and Carbonatites in South Mongolia.* Nauka: Moscow, Russia, 1983, 256 p. (In Russian)
50. Vladykin, N.V. Petrology and composition of rare-metal alkaline rocks in the South Gobi Desert (Mongolia). *Russ. Geol. Geophys*. **2013**, *54*, 545–568. https://doi.org/10.1016/j.rgg.2013.03.00.
51. Kuzmin, M.I.; Yarmolyuk, V.V. Mantle plumes of Central Asia (Northeast Asia) and their role in forming endogenous deposits. *Russ. Geol. Geophys.* **2014**, *55*, 120–143. https://doi.org/10.1016/j.rgg.2014.01.002.
52. Ripp, G.S.; Prokopyev, I.R.; Izbrodin, I.A.; Lastochkin, E.; Rampilov, M.O.; Doroshkevich, A.G.; Redina, A.A.; Posokhov, V.F.; Savchenko, A.A.; Khromova, E.A. Bastnaesite and Fluorite Rocks of the Ulan-Ude Occurrence (Mineral Composition, Geochemical Characteristics, and Genesis Issues). *Russ. Geol. Geophys.* **2019**, *60*, 1404–1424.
53. Warr, L. IMA–CNMNC approved mineral symbols. *Mineral. Mag.* **2021**, *85*, 291–320. https://doi.org/10.1180/mgm.2021.43.
54. Doroshkevich, A.G.; Kobylkina, O.V.; Ripp, G.S. The role of sulfates in formation of the West Transbaikalia carbonatites. *Dokl. Earth Sci.* **2003**, *388*, 535–539.
55. Andreeva, I.A.; Kovalenko, V.I. Magma compositions and genesis of the rocks of the Mushugai-Khuduk carbonatite-bearing alkaline complex (southern Mongolia): Evidence from melt inclusions. *Period. Mineral.* **2003**, *72*, 95–105.
56. Andreeva, I.A.; Kovalenko, V.I.; Naumov, V.B. Silicate-salt(sulfate) liquid immiscibility: A study of melt inclusions in minerals of the Mushugai-Khuduk carbonatite-bearing complex (southern Mongolia). *Acta Petrol. Sin.* **2007**, *23*, 73–82.
57. Redina, A.A.; Nikolenko, A.M.; Doroshkevich, A.G.; Prokopyev, I.R.; Wohlgemuth-Ueberwasser, C.; Vladykin, N.V. Conditions for the crystallization of fluorite in the Mushgai-Khudag complex (Southern Mongolia): Evidence from trace element geochemistry and fluid inclusions. *Geochemistry* **2020**, *80*, 125666**.** https://doi.org/10.1016/j.chemer.2020.125666.
58. Longerich, H.P.; Jackson, S.E.; Günther, D. Laser ablation inductively coupled plasma mass spectrometric transient signal data acquisition and analyte concentration calculation. *J. Analyt. Atom. Spect.* **1996**, *11*, 899–904.
59. Ulrich, T.; Günther, D.; Heinrich, C.A. The evolution of a porphyry Cu-Au deposit, based on LA-ICP-MS analysis of fluid inclusions: Bajo de la Alumbrera, Argentina. *Econ. Geol.* **2001**, *96*, 1743–1774.
60. Günther, D.; Audétat, A.; Frischknecht, R.; Heinrich, C.A. Quantitative analysis of major, minor and trace elements in fluid inclusions using laser ablation-inductively coupled plasma-mass spectrometry (LA-ICPMS). *J. Analyt. Atom. Spect.* **1998**, *13*, 263–270.
61. Veksler, I.V.; Petibon, C.; Jenner, G.A.; Dorfman, A.M.; Dingwell, D.B. Trace Element Partitioning in Immiscible Silicate–Carbonate Liquid Systems: An Initial Experimental Study Using a Centrifuge Autoclave. *J. Petrol.* **1998**, *39*, 2095–2104. https://doi.org/10.1093/petroj/39.11-12.2095.
62. Weidendorfer, D.; Schmidt, M.W.; Mattsson, H.B. A common origin of carbonatite magmas. *Geology* **2017**, *45*, 507–510. https://doi.org/10.1130/G38801.1.
63. Louvel, M.; Etschmann, B.; Guan, Q.; Testemale, D.; Brugger, J. Carbonate complexation enhances hydrothermal transport of rare earth elements in alkaline fluids. *Nat. Commun.* **2022**, *13*, 1456. https://doi.org/10.1038/s41467-022-28943-z.
64. Prokopyev, A.G.; Doroshkevich, A.E.; Starikova, Y.; Yang, V.O.; Goryunova, N.A.; Tomoshevich, V.F.; Proskurnin, V.A.; Saltanov, E.A. Kukharenko. Geochronology and origin of the carbonatites of the Central Taimyr Region, Russia (Arctica): Constraints on the F-Ba-REE mineralization and the Siberian Large Igneous Province. *Lithos* **2023**, *440–441*, 107045**.** https://doi.org/10.1016/j.lithos.2023.107045.
65. Stoppa, F.; Schiazza, M.; Rosatelli, G.; Castorina, F.; Sharygin, V.V.; Ambrosio, F.A.; Vicentini, N. Italian carbonatite system: From mantle to ore-deposit. *Ore Geol. Rev*. **2019**, *114*, 103041**.** https://doi.org/10.1016/j.oregeorev.2019.103041.
66. Buhn, B.; Rankin, A.H. Composition of natural, volatile-rich, Na-Ca-REE-Sr carbonatitic fluids trapped in fluid inclusions. *Geochim. Cosmochim. Acta* **1999**, *63*, 3781–3797.